applied sciences

MDPI

Article

Complex Research on Amorphous Vanadium Oxide Thin Films Deposited by Gas Impulse Magnetron Sputtering

Michał Mazur *, Aneta Lubańska, Jarosław Domaradzki and Damian Wojcieszak

Faculty of Electronics, Photonics and Microsystems, Wrocław University of Science and Technology, Janiszewskiego 11/17, 50-372 Wroclaw, Poland

* Correspondence: michal.mazur@pwr.edu.pl

Abstract: In this work, a complex examination of vanadium oxide thin films prepared by gas impulse magnetron sputtering with various Ar:O_2 gas ratios of 2:1 ÷ 8:1 was conducted. X-ray diffraction revealed the amorphous nature of the prepared thin films, and scanning electron microscopy images showed that the thin films were crack-free and homogenous. Optical properties investigations revealed that a higher oxygen content in the Ar:O_2 atmosphere during sputtering caused an increase in transparency. The sample prepared with the highest amount of oxygen in the gas mixture during deposition had 51.1% of the average transmission in the visible wavelength range. A decrease in oxygen caused deterioration in the thin film transparency with the lowest value equal to 21.8%. Electrical measurements showed that the prepared thin films had a semiconducting character with either electron or hole conduction type, depending on the sputtering gas composition. A small amount of oxygen in the gas mixture resulted in the deposition of p-type thin films, whereas an increase in the amount of oxygen caused a change to n-type electrical conduction. Resistivity decreased with increasing Ar:O_2 ratio. The gas sensing response toward diluted hydrogen was investigated for all the V_xO_y thin films, but at low operating temperatures, only the p-type thin films exhibited a visible response.

Keywords: vanadium oxide; magnetron sputtering; optical properties; electrical properties; p-type thin film; hydrogen gas sensing; hardness

Citation: Mazur, M.; Lubańska, A.; Domaradzki, J.; Wojcieszak, D. Complex Research on Amorphous Vanadium Oxide Thin Films Deposited by Gas Impulse Magnetron Sputtering. *Appl. Sci.* **2022**, *12*, 8966. https://doi.org/10.3390/app12188966

Academic Editors: Alessandro Fantoni and Heinz Christoph Neitzert

Received: 11 August 2022
Accepted: 4 September 2022
Published: 6 September 2022

1. Introduction

For many years, researchers have been searching for chemical compounds with good electrical properties as well as transparency in the visible wavelength range. It seems that some selected metal oxides such as V_xO_y, WO_x, In_xO_y, Co_xO_y or Ti_xO_y [1–3] are able to meet such requirements. Vanadium can occur in numerous oxidation states, e.g., V^{5+}, V^{4+} or V^{3+} which is advantageous for the preparation of thin films with different electrical and chemical properties for different applications [4]. Vanadium (di)oxide (VO_2) is known for its semiconductor-to-metal transition behaviour, which occurs at a specific temperature. Below 68 °C VO_2 is monoclinic, while above this temperature its structure changes to tetragonal rutile [5]. This structure transformation is fully reversible and is matched by a change in the optical and electrical properties of VO_2. Such behaviour makes VO_2 suitable, for example, for thermochromic applications [6,7]. V_2O_5 and V_2O_3 also exhibit a similar transition that occurs at temperatures of 250 °C and −120 °C, respectively [8]. Vanadium pentoxide (V_2O_5) is an n-type semiconductor with an optical band gap of 2.3 eV [9] and good thermal and chemical stability. It is used as a catalyst for chemical reactions [10]. Vanadia also has a potential application in chemoresistive gas sensors with oxidizing gases such as O_2 [11] or NO_x [12] or with reducing gases such as ethanol [13] or ammonia [14]. The low resistivity and high temperature coefficient of resistance (TCR) suggest potential applications in the construction of microbolometers [15]. Other possible applications of vanadium oxides are in smart windows [16], optical switches [17], infrared sensors [18] or flexible electronic devices [19].

To date, many methods have been used to prepare vanadium oxide thin films, for example sol-gel, evaporation, molecular beam epitaxy, or sputtering [18]. Magnetron sputtering seems to be one of the most interesting technologies because of the possibility to produce large area thin films with repeatable properties. The deposition process may be conducted at a low substrate temperature. The control of process parameters such as pressure or gas flow ratio allows us to obtain a high deposition rate and thin films with predictable properties [15]. It should be noted that in comparison with other deposition methods, magnetron sputtering has many advantages, e.g., very good adhesion to the substrate [20].

In recent years, there have been various reports regarding the properties of vanadium oxide thin films. Researchers have mainly focused on one form of oxide or methods of deposition other than magnetron sputtering. For example, Juan et al. [21] studied the thermochromic properties of vanadium dioxide (VO_2) deposited by high-power impulse magnetron sputtering. The deposition process was carried out using various reactive and working gas ratios ranging from 10:1 to 100:1 for Ar:O_2. It should be noted that as-deposited thin films were further annealed at 500 °C for 3 min which resulted in formation of the crystalline structure. The addition of a TiO_2 buffer layer between VO_2 and the substrate caused an increase in crystallinity and a higher transparency of thin films. The authors showed that with the decrease in the Ar:O_2 ratio, the crystal phase changed from V_2O_3 to VO_2 and finally to V_2O_5. Furthermore, TEM investigations showed that as-deposited thin films became amorphous with lower Ar:O_2 gas ratios [21]. In turn, Bukhari et al. [22] compared the influence of various oxygen flow rates during the deposition of VO_2 using a pulsed laser deposition technique on resistivity and transition temperature. Seven sets of thin films were deposited using various oxygen flow rates ranging from 0.5 to 90 sccm while maintaining a constant background pressure. The authors showed that at low oxygen flow rates, i.e., 0.5 sccm and 1 sccm, very small crystalline islands were created on the substrate, whereas an increase in the flow rate caused an increase in the crystallites size because of the better surface diffusion. In this case, the flow rate influenced the surface roughness parameters. Vanadium oxide thin films deposited with higher oxygen content showed two orders of change in resistance as a function of temperature. It was discussed that the grain size affects the nucleation effects, which in turn leads to a change in the transition temperature and can be observed in electrical measurements [22]. Furthermore, Fieldhouse et al. [23] compared the electrical properties of vanadium oxide thin films prepared by magnetron sputtering with various O_2 contents in the gas mixture during preparation (5, 7.5, 10, 15%) and different substrate temperatures. The authors observed a correlation between the electrical properties of the sputtered V_xO_y samples and the deposition conditions. The thin films deposited at higher O_2 content were shown to be amorphous. The resistivity of the samples increased with increasing partial oxygen pressure during the preparation process from 0.02 to 100 Ωcm. Moreover, higher resistivity caused an increase in the activation energy values calculated from the Arrhenius equation. Those values ranged from 0.04 to 0.24 eV, and this behaviour was correlated with the electrical charge transport energy. The prepared vanadium oxides exhibited the Meyer–Neldel rule of charge transport mechanism: invert or conventional depending on the O_2 pressure and substrate temperature during magnetron sputtering [23]. In turn, Luo et al. [24] discussed the microstructure, electrical and optical properties of as-deposited and annealed V_xO_y thin films prepared by magnetron sputtering with a low O_2:Ar flow ratio. Measurements of the optical properties revealed that the as-deposited thin film had an absorption edge at ca. 400 nm. The authors pointed out that prepared V_xO_y thin films are desired as thermal sensing materials based on their high TCR value (2.0–3.1%/°C) [24]. Jang et al. [25] discussed the influence of oxygen partial pressure on the properties of vanadium oxide thin films deposited by magnetron sputtering with different argon to oxygen gas mixtures and pure oxygen. The argon flow rate was constant and equal to 20 sccm while the oxygen values were 1, 3 and 5 sccm. Analysis of the X-ray diffraction spectra showed that all the deposited samples were amorphous, while those deposited

with an oxygen flow rate of 3 sccm and above had a lamellar structure. The samples prepared with a higher oxygen content exhibited gasochromic properties and are potential candidates for hydrogen gas sensors [25]. Koussi et al. [26] examined vanadium dioxide prepared by pulsed laser deposition and rapid thermal annealing. The authors focused on producing a good quality thin film that exhibited the semiconductor-metal phase transition. They produced thin films using various substrates and showed that the control of the annealing temperature causes a change in transition temperature. The authors obtained vanadium dioxide with a thickness of 25 nm and a transition temperature equal to 52 °C on both quartz and silicon substrates, which is an achievement compared with the usual transient temperature of 68 °C [26]. According to Li et al. [27], atomic layer deposition leads to the fabrication of amorphous vanadium oxide, while the annealing of the as-deposited samples leads to the phase transition to crystalline structures. Scanning electron microscope images showed a smooth and uniform surface of as-deposited thin films. The authors showed that atomic layer deposition allowed the production of vanadium oxides with good thermochromic properties [27]. According to the literature [28], the control of technological parameters e.g., gas partial pressure, supply power, or substrate temperature affects morphology, stoichiometry and electrical properties. Changes in microstructure due to various substrate temperatures or pressures in the chamber during magnetron sputtering are widely described by the Thornton Model where the properties of Ti-doped Cu3N were described [29]. The authors showed that maintaining the substrate at room temperature during magnetron sputtering results in deposition of columnar oriented grain growth or amorphous thin films, and an increase in the substrate temperature results in a crystalline structure. This behaviour is related to the surface mobility of ad-atoms [28,29].

In this paper, seven sets of vanadium oxides were deposited by gas impulse magnetron sputtering using different Ar:O_2 ratios ranging from 2:1 to 8:1. The gas impulse magnetron sputtering, based on the sequential injection of gas directly at the target surface, has recently gained attention. In this process, the pressure during sputtering is reduced, decreasing the number of collisions of ions, the energy loss of the sputtered particles reaching the substrate and simultaneously causing the elongation of the mean free path of the sputtered ions. Furthermore, the repeatable ignition of the glow discharge results in a thermal disequilibrium of the plasma leading to the deposition of thin films with different properties compared with those sputtered in a standard process. The research conducted here clearly shows that the control of the working gas ratio during magnetron sputtering makes it possible to obtain amorphous vanadium oxide thin films with various optical, electrical, gas sensing, and mechanical properties, which may be optimized in this way due to their potential application. In particular, it was shown that with suitable changes in the sputtering atmosphere, it was possible to deposit vanadium oxide thin films with hole or electron type of conduction that influenced its gas-sensing properties at low operating temperatures.

2. Materials and Methods

Vanadium oxide thin films were deposited using the gas impulse magnetron sputtering method using a high purity metallic vanadium target (99.99%). The pressure during deposition was kept constant at ca. $5 \cdot 10^{-3}$ mbar. The target-substrate distance was equal to 160 mm. The gas was injected directly over the target area using a fast valve (Festo) with a frequency of 10 Hz and each gas pulse lasted for 30 ms. This in turn caused repeatable ignition of the glow discharge because the powering of the magnetron source was electronically synchronized with each gas pulse. After each pulse, the power supply was cut, causing a 70 ms break of the glow discharge. The frequency of the gas impulse and the pulse width were precisely set at these values to ensure the stability of the sputtering process and a reasonable deposition rate of the thin films. For the sputtering process, a medium frequency power supply (165 kHz) was used with a voltage amplitude of 1.8 kV. Seven sets of vanadium oxide thin films were deposited and each set was prepared in different Ar:O_2 gas ratios ranging from 2:1 to 8:1. The duration of the sputtering

process was adjusted to obtain thin films with a similar thickness, i.e., in the range from 310 nm to 340 nm. The thin films were deposited on various substrates, including polished silicon, fused silica, and alumina substrates. The alumina substrates were purchased from BVT Company (Czech Republic) and were composed of corundum ceramic base and interdigitated structures of electrodes made of platinum-gold alloy applied on their surface. The substrate dimensions were as follows: 25 mm in length, 7 mm in width, and 0.6 mm thickness.

The microstructure of the thin films was evaluated based on X-ray diffraction measurements performed in the grazing incidence mode using the Empyrean PANalytical X-ray diffractometer equipped with a PIXel3D detector and CuKα X-ray source with a wavelength of 1.5406 Å. It is worth mentioning that XRD measurements were conducted in a grazing incidence mode, which is more useful for very thin samples and is more surface sensitive since wave penetration is limited. The measurements were carried out in the 2θ range of 30 to 80° with a step of 0.05° and a time per step of 5 s with an incidence angle of X-ray radiation of 3° relative to the sample surface. For such low incidence angles, it is possible to measure the structural properties of very thin layers at the surface.

The surface morphology and cross-section studies were performed using the SEM/Xe-PFIB FEI Helios scanning electron microscope equipped with an EDAX energy dispersive spectroscopy detector, which was used for the qualitative analysis of the material composition of the thin films.

The optical properties were assessed on the basis of the light transmission spectra measured in the wavelength range of 300–1000 nm using an Ocean Optics QE65000 spectrophotometer and a Mikropack DH-BAL 2000 light source. The fundamental absorption edge and the optical energy band gap were determined for each set of thin films.

The current-voltage characteristics and Arrhenius plots were obtained using the Keithley SCS4200 characterization system and a M100 Cascade Microtech probe station, and were used to calculate the sheet resistance and resistivity of as-deposited thin films. The temperature-dependent resistivity measurements were performed in the temperature range of 300 K to 350 K and were used for the calculation of the activation energy.

Based on the obtained optical and electrical data, the deposited vanadium oxide thin films were compared using the figure of merit (Q) coefficient calculated according to the following equation:

$$Q = \frac{T^{10}}{\rho} \quad (1)$$

where T is the average optical transmission in the visible wavelength range, and ρ is the resistivity at room temperature (Ωcm).

Determination of the figure of merit allows a comparison of the performance of TCO or TOS coatings on the basis of their transparency and electrical resistance. The method of determining the figure of merit coefficient, proposed by the authors, uses the relationship between the average transparency in the visible wavelength range (i.e., the range from 380 to 760 nm) and the resistivity of the thin films. In this way, the figure of merit for visible light is determined and made independent of thin film thickness by the use of resistivity.

The gas sensing properties of the as-deposited vanadium oxides were examined in a chamber where samples were placed on a heating stage and exposed to diluted hydrogen in argon (3.5%). The temperature of the gas sensing process was controlled by the Instec mK1000 temperature controller, and before the measurements, the samples were stabilized at the operating temperature for an hour. Agilent 34970A data acquisition systems were used to determine the resistance change.

The hardness of the vanadium oxides was measured with the aid of a CSM Instruments nanoindenter equipped with a diamond Vickers tip.

3. Results and Discussion

The deposition rate was calculated based on thickness of the deposited thin films and the time of the sputtering process (Figure 1). As is clearly shown, the lower the oxygen content in the gas mixture ratios, the higher the deposition rate obtained and the dependence of the deposition rate on the Ar:O_2 ratio was almost linear. This behaviour is caused by the higher incident energy of the Ar ions compared with the O_2 ions. This, in turn, increases the sputtering rate of the target, resulting in the deposition of thin films with the same thickness but in a shorter time.

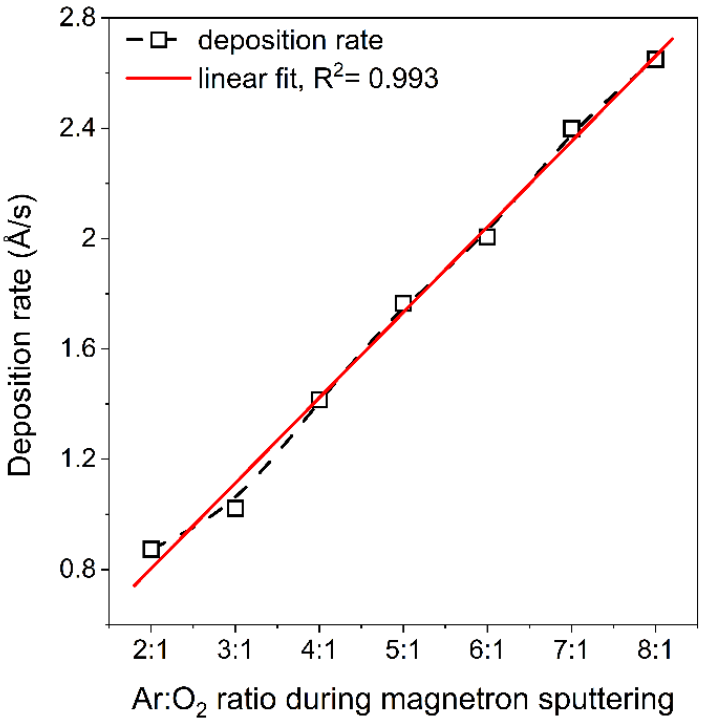

Figure 1. Dependence of the deposition rate of vanadium oxides thin films on the Ar:O_2 gas ratio during magnetron sputtering.

3.1. Structure and Surface Morphology

The XRD patterns of the as-deposited thin films are shown in Figure 2. All the thin films were amorphous, which might be related to the low temperature of the sputtering process and long target-substrate distance; therefore, the particles reaching the substrates had low energy not sufficient for the nucleation of a crystalline structure. Other similar results have been presented for vanadium oxide thin films deposited by magnetron sputtering without additional annealing, e.g., [23–25]. Moreover, in the case of tungsten oxides thin films deposited by the same gas impulse magnetron sputtering method, the results of the XRD measurements also showed that they were amorphous [30]. In this way, further analysis of other properties does not depend on the microstructure of the thin films but rather on the sputtering atmosphere during the deposition process. It is also worth mentioning that amorphous thin films should exhibit better optical properties, e.g., transmission coefficient, compared with those of the crystalline thin films.

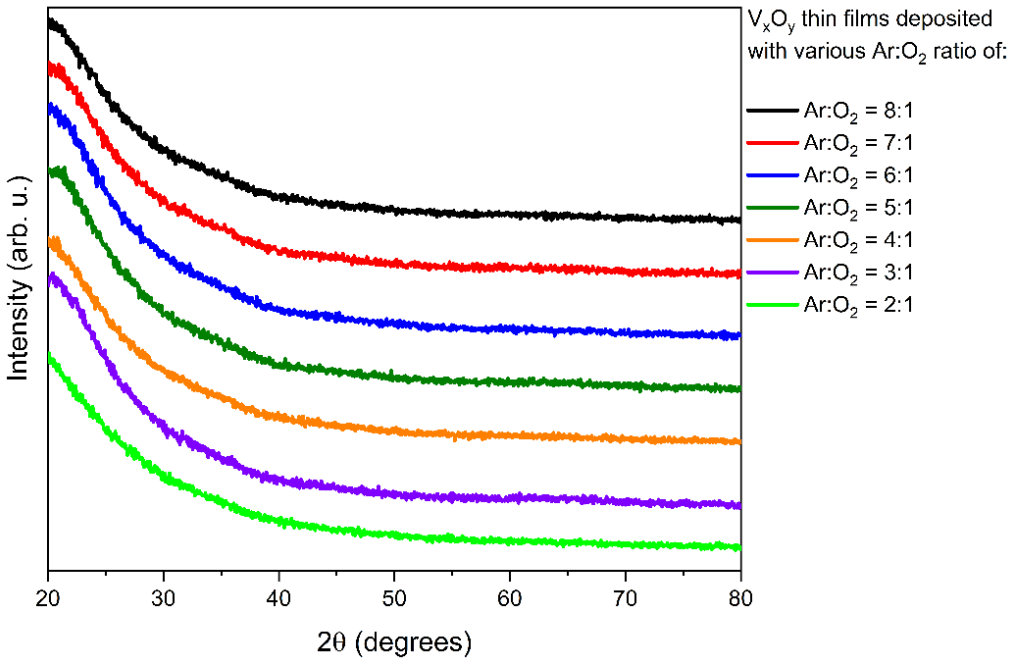

Figure 2. Diffraction patterns of vanadium oxides deposited with various Ar:O_2 gas ratios.

The SEM images in Figure 3 show the surface morphology of the as-deposited vanadium oxide thin films. Thin films deposited with Ar:O_2 ratios between 8:1 and 6:1 are smooth, uniform, crack-free and composed of very small nanograins. A further increase in the oxygen content in the sputtering atmosphere resulted in an increase in grain size (Figure 3d–f), but the thin films were still homogenous and crack-free. In contrast, the sample deposited with an Ar:O_2 ratio of 2:1 was inhomogenous, rather rough, and composed of grains of various sizes. The EDS spectrum measured for a vanadium oxide thin film deposited with an Ar:O_2 ratio of 4:1 is shown in Figure 3h and has peaks for vanadium and oxygen related to the material composition of the film and for silicon, which is the substrate material. Since the thickness of the vanadium oxide thin film is approximately 320 nm, the silicon peak of the Kα line (at 1.74 keV) is large and visible because the penetration depth of the EDS beam is also large. No other peaks related to the other elements were found, indicating good purity of the deposited coatings.

3.2. Optical Properties

The optical properties of the V_xO_y thin films were examined on the basis of the transmission characteristics shown in Figure 3. A higher oxygen content in Ar:O_2 gas ratios during sputtering caused an increase in the average transmission coefficient in the visible wavelength range. The characteristics of films prepared with the Ar:O_2 ratios of 2:1 and 3:1 are almost overlapped, i.e., the average transmission is c.a. 2% higher for the sample prepared with a higher oxygen content. Moreover, these films had the same thickness of 325 nm and were transparent. A decrease in oxygen content in the gas mixture during sputtering caused a further decrease in the transparency of the thin films. The dependence of the average transmission determined in the visible wavelength range on the Ar:O_2 gas ratio is presented in Figure 4. It was calculated using the integral of each transmission characteristic in the range of 380 nm to 760 nm. The average transmission values are almost the same for three sets of thin films prepared with the highest oxygen content and range between 48.6% and 51.1%. The decrease in oxygen in the gas atmosphere during the deposition process caused the decrease in average transmission to 36.2% and 39.1% for samples deposited with 6:1 and 5:1 Ar:O_2, respectively. A further decrease in the O_2 content in the gas mixture during magnetron sputtering caused the decrease in the average transmission values to 21.8% and 24.5% (Figure 4, Table 1). According to the

literature, similar research on vanadium oxides was conducted by Castro et al. [31], who studied V_xO_y thin films deposited with different oxygen partial pressure and substrate temperature during the deposition process. They showed that thin films prepared at room temperature with low oxygen partial pressure (from 0.5 to 1%) had a yellow to dark green colour and were amorphous, as observed in this work. Other authors, e.g., Tashtoush et al. [32], compared V_2O_5 with different thicknesses of 320, 550 and 700 nm and showed that thicker films had lower transmission coefficients, i.e., 73%, 58% and 45%, respectively [32]. Ghanashyam et al. [33] focused on the vanadium oxide examination by comparing various thicknesses and oxygen partial pressure during the magnetron sputtering process. They found that a higher oxygen partial pressure resulted in a higher transmission rate, and that a change of three orders caused an increase from approximately 62% to 78%. Furthermore, a higher transmission was observed once more for thinner thin films [33]. Ramana et al. examined the influence of V_2O_5 grain size on the transmission coefficient and reported values in the range of 66% to 75%, where higher grain size resulted in lower transmission [34].

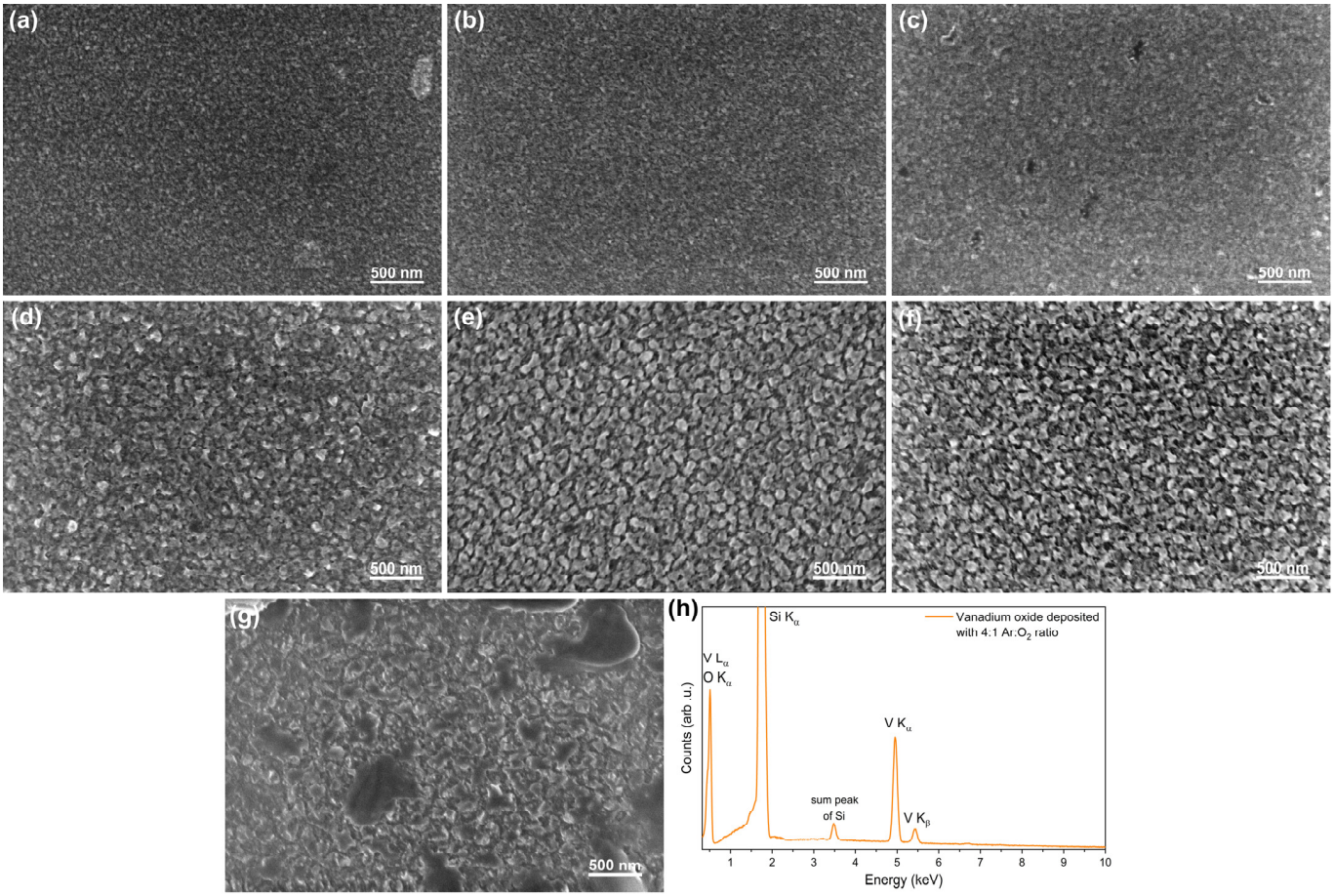

Figure 3. SEM images of the surface morphology of vanadium oxide thin films deposited with various $Ar:O_2$ gas ratios: (**a**) 2:1, (**b**) 3:1, (**c**) 4:1, (**d**) 5:1, (**e**) 6:1, (**f**) 7:1, (**g**) 8:1 and (**h**) an EDS spectrum of a thin film deposited with $Ar:O_2$ ratio of 4:1.

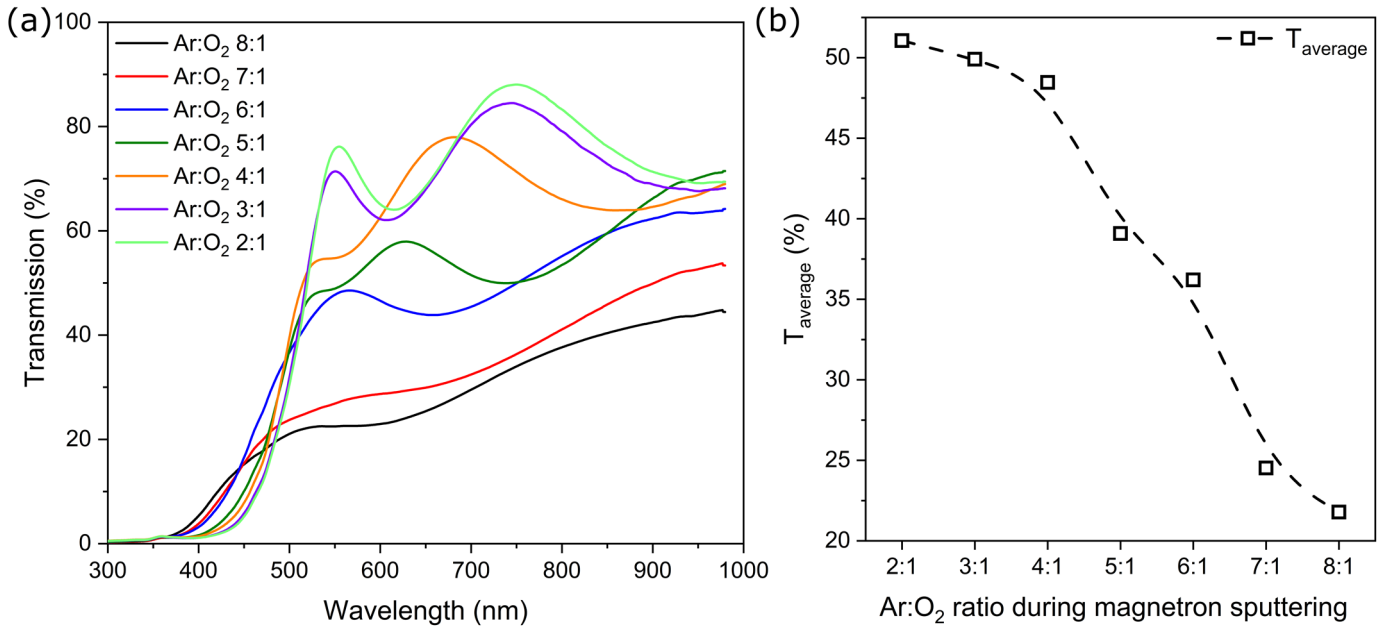

Figure 4. Results of: (**a**) transmission spectra of V_xO_y thin films deposited with various $Ar:O_2$ gas ratios during the magnetron sputtering process and (**b**) the average transmission of vanadium oxides in the VIS wavelength range.

Table 1. Summary of the properties of deposited vanadium oxide thin films prepared with various $Ar:O_2$ gas ratios during magnetron sputtering.

$Ar:O_2$ Ratio	Deposition Rate (Å/s)	Average Transmission (%)	$\lambda_{cut\text{-}off}$ (nm)	E_g (eV)	Sheet Resistance (Ω/□)	Resistivity (Ωcm)	Q
8:1	2.68	21.8	371	2.01	$2.99 \cdot 10^5$	9.10	$2.64 \cdot 10^{-8}$
7:1	2.46	24.5	386	1.91	$2.06 \cdot 10^6$	$6.70 \cdot 10^1$	$1.17 \cdot 10^{-8}$
6:1	2.01	36.2	405	1.99	$3.42 \cdot 10^6$	$1.11 \cdot 10^2$	$3.48 \cdot 10^{-7}$
5:1	1.79	39.1	447	2.00	$6.23 \cdot 10^6$	$2.28 \cdot 10^2$	$3.64 \cdot 10^{-7}$
4:1	1.42	48.5	454	2.06	$6.98 \cdot 10^6$	$2.16 \cdot 10^2$	$3.31 \cdot 10^{-6}$
3:1	1.02	49.9	466	2.07	$9.44 \cdot 10^6$	$3.07 \cdot 10^2$	$3.12 \cdot 10^{-6}$
2:1	0.87	51.1	470	2.08	$7.14 \cdot 10^7$	$2.04 \cdot 10^3$	$5.90 \cdot 10^{-7}$

The fundamental absorption edge was calculated from the transmission spectra. The values are red-shifted with the higher O_2 content in the sputtering atmosphere (Figure 5). The values of $\lambda_{cut\text{-}off}$ range between 371 and 470 nm (Table 1). Benmoussa et al. [35] reported the fundamental absorption edge at about 600 nm, while other authors reported values between 460 and 550 nm [36–39] for amorphous V_2O_5 thin films prepared using magnetron sputtering.

Additionally, the optical band gap energy (E_g) was calculated using Tauc plots (Figure 6) [31,40]. The values did not vary significantly and were in the range between 1.91 and 2.08 eV. According to the literature [41], various factors may affect the energy band gap of vanadium oxide, for example, the deposition method, the thickness of the thin film or the type of substrate [33,42–45]. Similar values of the energy band gap have been obtained in the literature [44], where the authors studied annealed V_2O_5 at various temperatures. The results ranged from 2.32 to 1.98 eV with increasing temperature. The authors pointed out that thin films prepared at room temperature were stoichiometric, whereas at elevated temperatures they were substoichiometric. Ramana et al. [46] concluded that an increase in the deposition temperature causes a decrease in the optical energy band gap due to the formation of oxygen ion vacancies. However, heat treatment in O_2 caused an increase in band gap energy and transmission coefficient due to the partial filling of the vacancies. Other

authors confirmed that a higher deposition temperature causes a decrease in optical band gap energy [43], but there are also reports that point to the opposite behaviour [47]. Other authors [32] reported an optical band gap energy equal to 1.87 and 2.1 eV for amorphous V_2O_5 with different thicknesses, which is also in agreement with the results reported here.

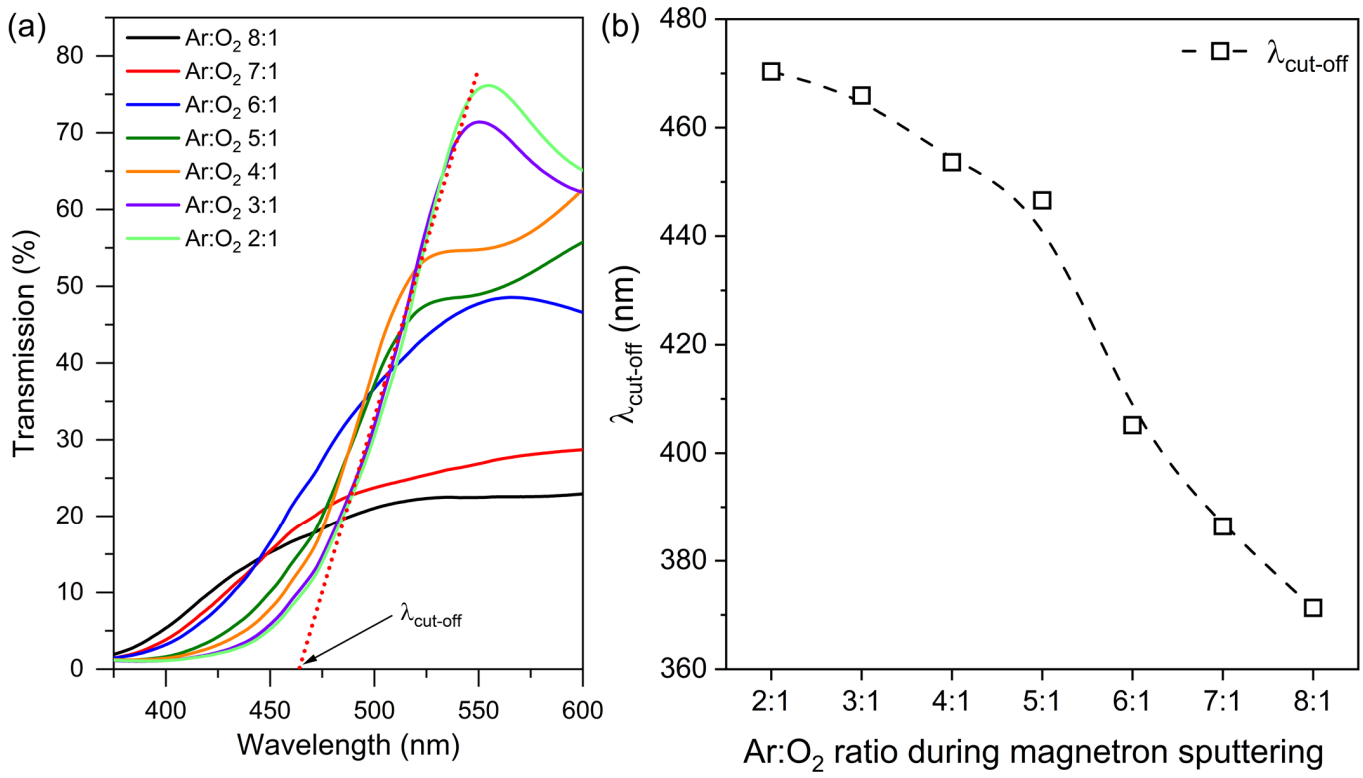

Figure 5. Results of (**a**) the determination of the fundamental absorption edge on a sample prepared with 2:1 Ar:O_2 gas ratio during magnetron sputtering and (**b**) dependence of the fundamental absorption edge on the Ar:O_2 gas ratio during sputtering.

3.3. Electrical Properties

The current-voltage characteristics of the selected thin films recorded in a planar configuration using alumina substrates containing interdigitated electrodes are shown in Figure 7. These thin films were selected due to their resistance change in relation to the other samples, and more precisely, the Ar:O_2 gas ratios for which there was a more visible change in resistance of the films. All the graphs show the linear dependence of current and voltage, which indicates the ohmic behaviour of prepared thin films. The slope of the relationship changes with changes in the resistance of the thin films; i.e., it was greater for the thin films deposited with less oxygen in the gas mixture during sputtering, meaning that these films are less resistive.

The resistivity as a function of temperature is shown in Figure 8. The resistivity values decrease as the temperature increases for each deposited vanadium oxide. The highest resistivity was obtained for the sample prepared with the 2:1 Ar:O_2 gas ratio during the deposition process. The decrease in oxygen content in the sputtering atmosphere caused a three-fold decrease in resistivity values for samples deposited with Ar:O_2 of 8:1. Similar examinations were conducted by Dong et al. [46], who compared vanadium oxides deposited with different oxygen flow rates and duty cycles. It was shown that the resistivity of the samples increases with an increase of the O_2 flow rate. Furthermore, the authors observed that the morphology, the deposition rate, and the electrical properties strongly depend on the oxygen content during the deposition process [46].

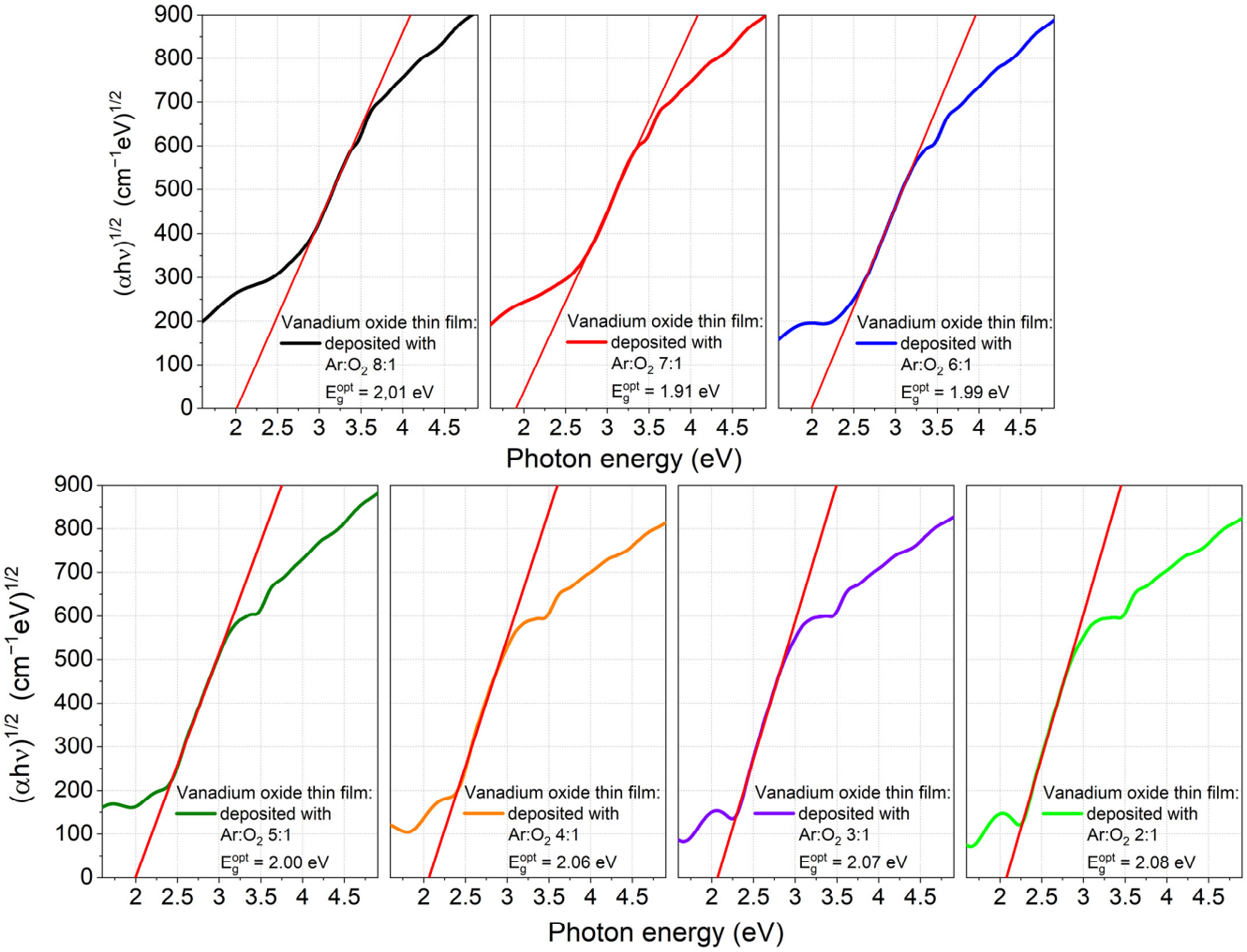

Figure 6. The fundamental absorption edge of as-deposited vanadium oxide thin films.

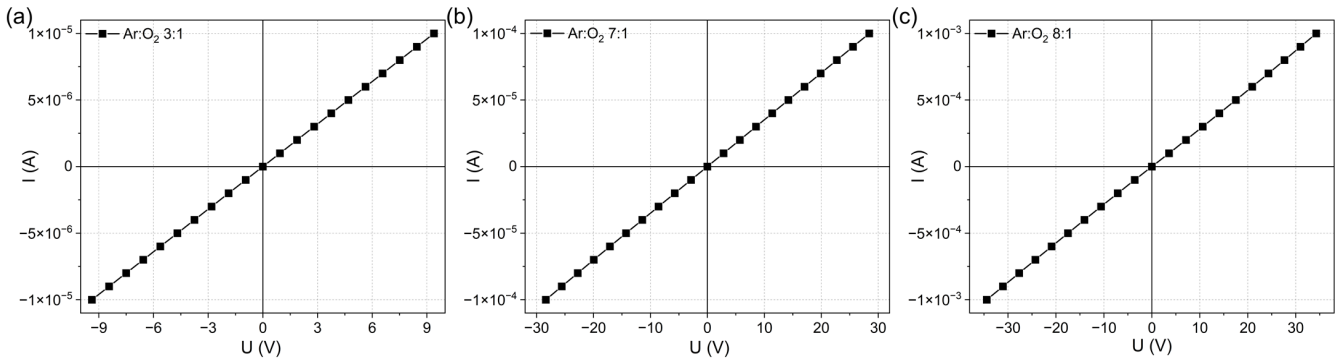

Figure 7. Current-voltage characteristics of selected V_xO_y thin films prepared with $Ar:O_2$ gas ratios of: (**a**) 3:1, (**b**) 7:1 and (**c**) 8:1.

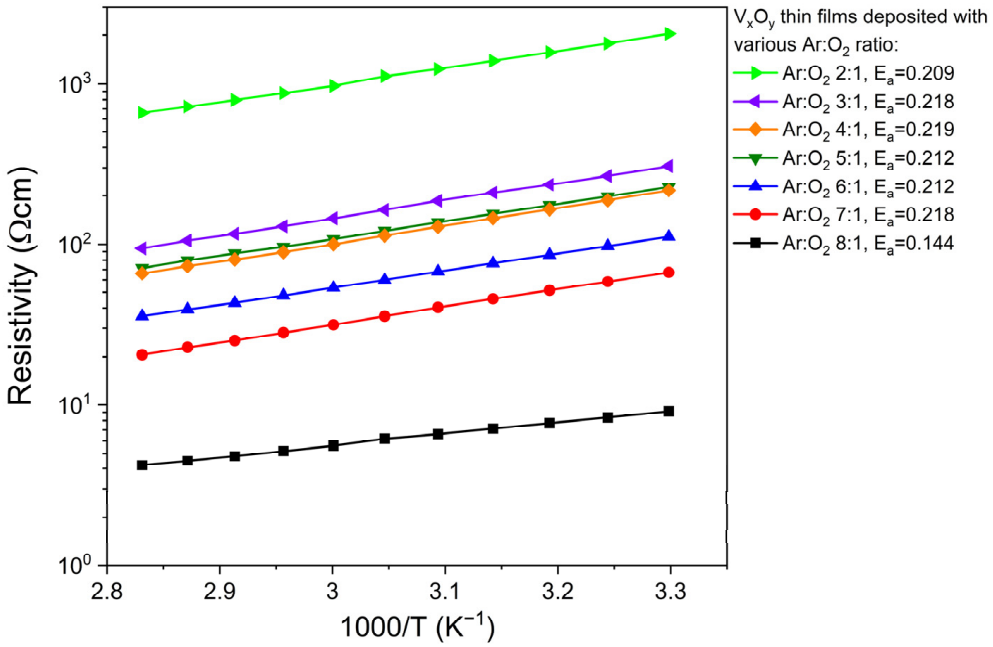

Figure 8. Resistivity as a function of 1000/T of vanadium oxide thin films deposited with various Ar:O_2 gas ratios during sputtering process.

The activation energy (E_a) was calculated for each sample based on the Arrhenius law (2) and linearly-fitted slopes of the resistivity as a function of the temperature plots, using the following equation [48]:

$$\rho = \rho_0 exp\left(\frac{E_a}{kT}\right) \quad (2)$$

where k is the Boltzmann constant and T is the absolute temperature.

The thermal activation energy has the lowest value (0.144 eV/K) for V_xO_y film prepared with the 8:1 Ar:O_2 gas ratio. The E_a values calculated for the remaining thin films were almost the same, ranging between 0.209 and 0.219 eV/K. Similar results were obtained by M. Öksüzoğlu et al. [49] for the V_2O_5 measured in the temperature range between 50 and 100 °C. The authors stated that as-deposited vanadium pentoxide was amorphous and had two ranges of thermal activation energy for the temperatures of 25–50 °C and 50–100 °C, which related to the thermal activation of electrical charge carriers into the conduction band and the change in the number of charge carriers in the conduction band, respectively. The optical energy gap was shown to affect electrical properties, such as the activation energy of V_2O_5 deposited with pulsed DC magnetron sputtering [49].

The dependence of the resistivity and sheet resistance of vanadium oxide thin films on the Ar:O_2 gas ratio during the deposition process is presented in Figure 9. Both resistivity and sheet resistance increase with increasing amounts of oxygen in the Ar:O_2 gas mixture. The values are in the range of 9.10 to $2.04 \cdot 10^3$ Ωcm. Analogous results were obtained by Choi et al. [50] who showed that the sheet resistance and resistivity of amorphous V_2O_5 increase with the increases in the amount of oxygen in the sputtering gas ratio. Researchers showed that proper control of the oxygen flow rate enables adjustments to some properties of vanadium pentoxide, e.g., electrical properties or stoichiometry [50].

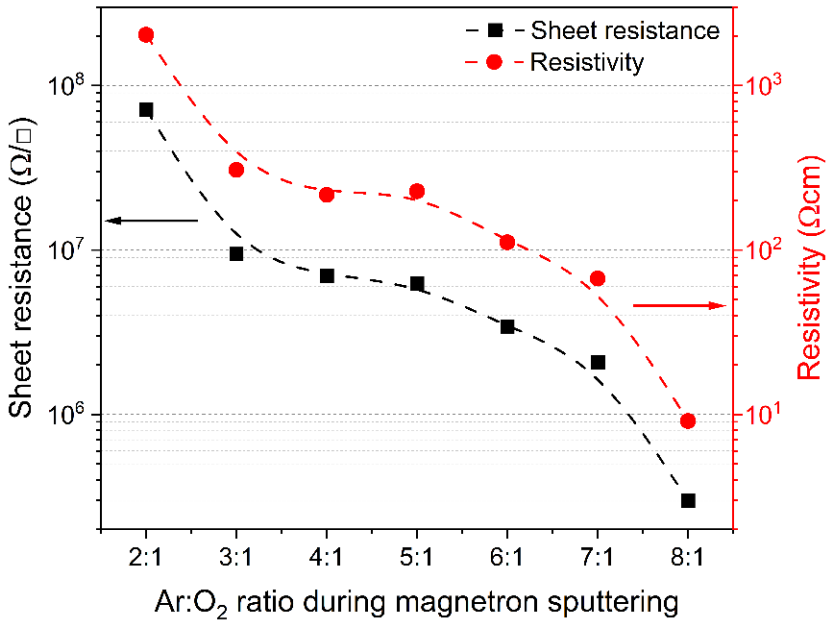

Figure 9. Dependence of sheet resistance and resistivity of vanadium oxide thin films on the $Ar:O_2$ gas ratio during the preparation process.

In addition, to compare the optical and electrical properties of analysed vanadium oxide thin films deposited with different $Ar:O_2$ ratios during sputtering, the merit figure (Q) was calculated based on the average transmission in the visible wavelength range and resistivity values (Equation (1)), for each sample. The calculated values of the merit figure are in the range from $2.64 \cdot 10^{-8}$ to $3.31 \cdot 10^{-6}$ and the dependence of Q on the $Ar:O_2$ gas ratios during sputtering is shown in Figure 10. The thin films deposited with $Ar:O_2$ gas ratios of 3:1 and 4:1 were found to have the highest Q values. This was related to the high average transmission, which was very similar to the V_xO_y deposited with $Ar:O_2$ gas ratio 2:1, and at the same time resulted in a one-order lower value of resistivity compared to the mentioned sample. Thin films deposited with a gas ratio greater than 4:1 had significantly lower average transmission, which led to a decrease in the Q factor.

The Seebeck coefficient (S_c) of the prepared thin films was determined on the basis of thermoelectric measurements (Figure 11). The characteristics of the thermoelectric voltage as a function of the temperature difference between electrical contacts for all the deposited vanadium oxide thin films are presented in Figure 9. The positive sign of the Seebeck coefficient indicates the hole type of electrical conduction, while the negative sign indicates the electron type [51]. Samples prepared with the lowest oxygen content in $Ar:O_2$ gas ratios, i.e., 8:1, 7:1 and 6:1, were p-type semiconductors, whereas those prepared with ratios below 6:1 were n-type semiconductors. Therefore, a lower O_2 content in the $Ar:O_2$ gas mixture resulted in a p-type of electrical conduction that could be an effect of the oxygen vacancies present in the microstructure of the film. The oxygen vacancies were also responsible for the deterioration of the average transmission in the visible-wavelength range of deposited thin films and an increase in their conductivity. Similar behaviour of optical and electrical properties has been already reported for non-stoichiometric WO_x thin films prepared by magnetron sputtering [30]. As the sputtering atmosphere became more oxygen rich, the conduction switched to the electron type, which was related to a lower number or even an absence of oxygen vacancies. The thermoelectric characteristics with calculated S_c are presented in Figure 9.

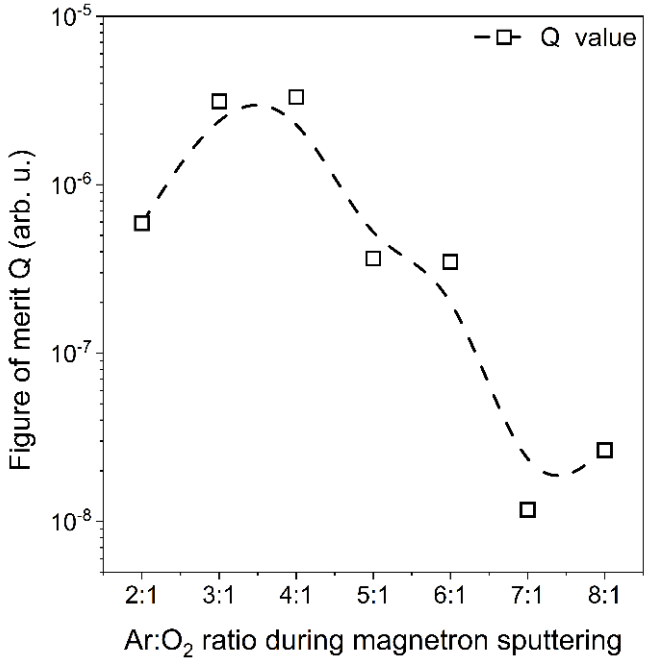

Figure 10. Dependence of the figure of merit of vanadium oxide thin films on the Ar:O_2 gas ratio during the magnetron sputtering process.

The summary of optical and electrical properties of as-deposited vanadium oxide thin films is shown in Table 1.

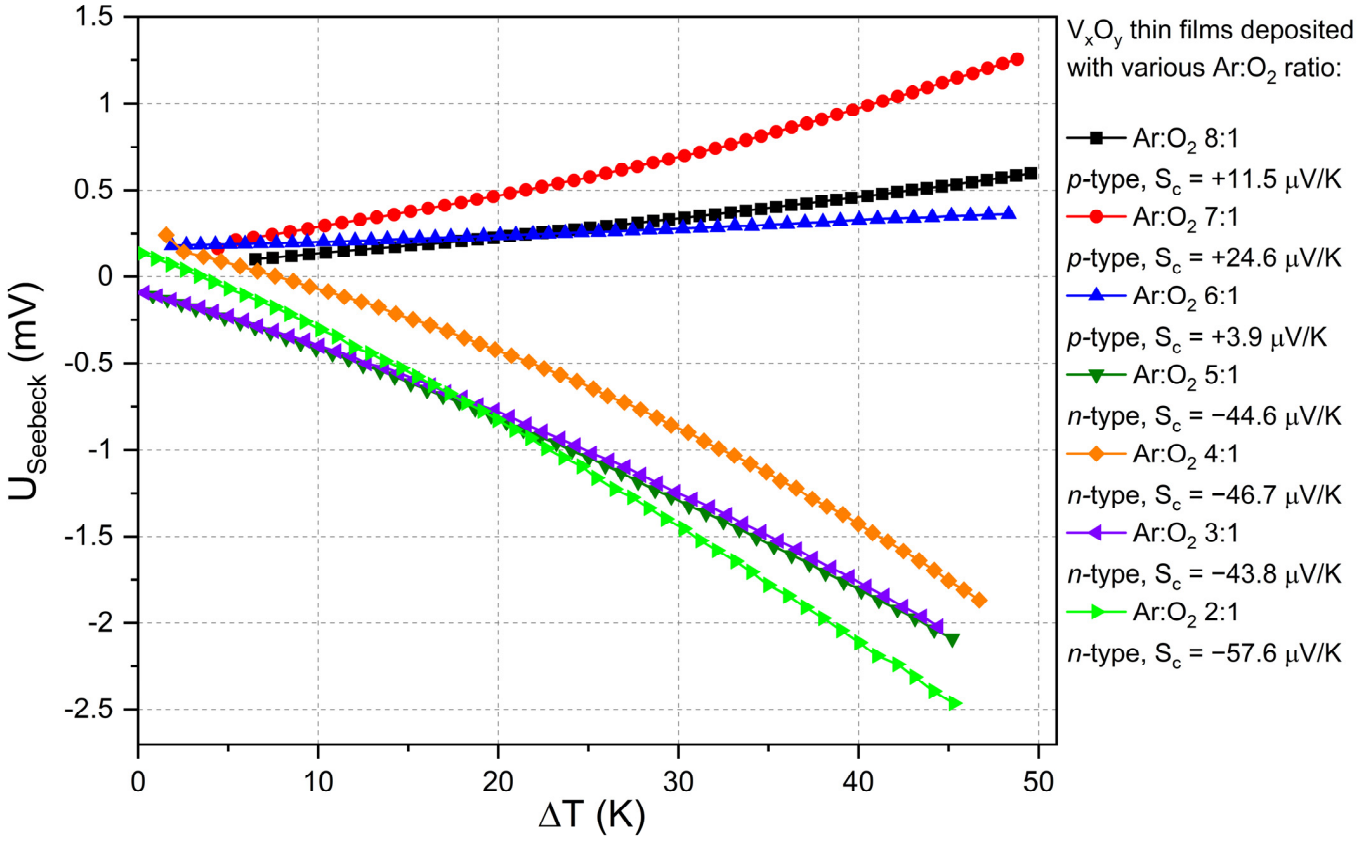

Figure 11. Thermoelectric characteristics of vanadium oxides thin films deposited with various Ar:O_2 gas ratios.

3.4. Gas Sensing Properties

Due to the semiconducting character of the thin films, their gas sensing properties towards 3.5% hydrogen diluted in argon were examined. Changes in resistance after gas exposure as a function of time are shown in Figure 12. The gas-sensing mechanism of chemoresistive gas-sensing layers is correlated with oxygen vacancies created at the surface of the sensing film during exposure to the temperature. When exposed to air, oxygen is physisorbed on free states on the sensor surface at room temperature. As the temperature increases, O_2 molecules chemisorb in the previously physisorbed layer and trap conduction charges from the deeper part of the thin film, which causes the formation of oxygen ions on the surface (the oxidation state and reactivity of which depend on the temperature) and the resistance of the film increases or decreases depending on the type of semiconductor. When the sensing film is placed in the gas atmosphere, the resistance behaviour reverses after the adsorption of the gas molecules. The resistance changes are related to the bending of the Fermi level as a result of the formation of a depletion or enhancement region. After exposure to the ambient atmosphere, the resistance returns to the starting level before exposure to the gas. The sensing performance may be improved by adding noble dopants such as Pd or Au [52,53].

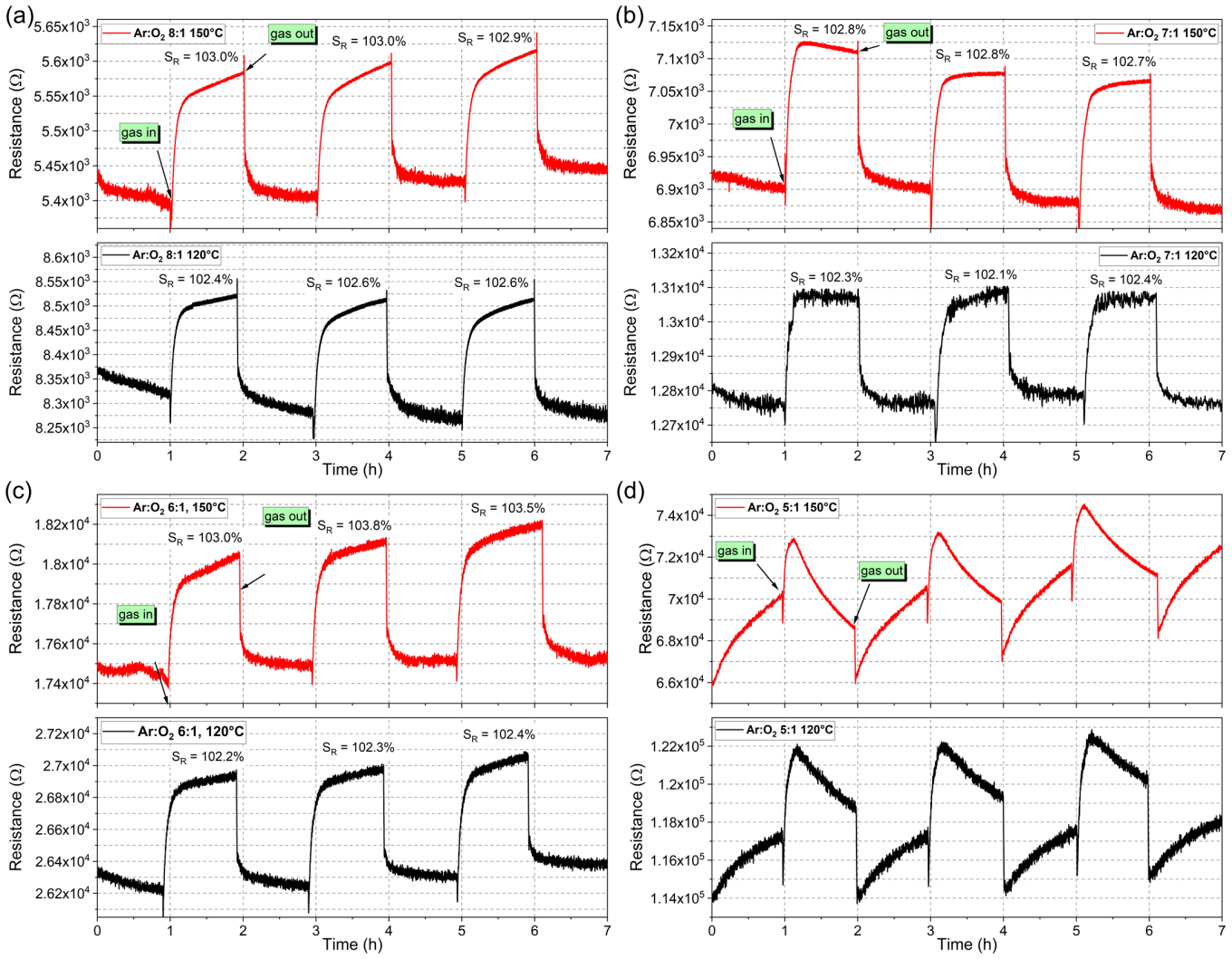

Figure 12. Gas response upon exposure to the 3.5% of hydrogen of as-deposited V_xO_y thin films prepared using various Ar:O_2 gas ratios during sputtering: (**a**) 8:1, (**b**) 7:1, (**c**) 6:1, (**d**) 5:1.

According to the literature, a better sensing response toward hydrogen is exhibited by *n*-type semiconductors. The sensor response of the *p*-type semiconducting thin film is usually lower and is defined as the square root of the same n-type thin film (3) [54–56]. H_2 molecules interact with the surface as protons, then desorb as water vapour and again interact as hydroxyl ions. The detection of hydrogen using a *p*-type semiconductor is described by Equations (4) and (5) [57–59].

$$S_p = \sqrt{S_n} \tag{3}$$

$$2H_2 + O^-_{2(adsorbed)} \leftrightarrow 2H_2O + e^- \tag{4}$$

$$H_2O \leftrightarrow OH^- + H^+ \tag{5}$$

The sensor response was investigated for all deposited thin films, but only the results are shown for those prepared with 8:1, 7:1, 6:1 and 5:1 Ar:O_2 gas ratios during magnetron sputtering. A better sensor response was obtained for the *p*-type thin films (Figure 10) compared with the *n*-type, which were difficult to determine. The investigations were carried out at two operating temperatures: 120 °C and 150 °C. The characteristics of resistance changes as a function of time resemble a typical gas response graph for *p*-type semiconducting oxides [60,61]. For other *n*-type semiconducting vanadium oxide thin films, i.e., prepared with Ar:O_2 gas ratio of 5:1 and lower, the gas response characteristics were analogous to those in. It was impossible to determine gas response or response/recovery times due to the low operating temperature and the amorphous structure of the *n*-type thin films that results in a very low active surface area.

The summary of the gas sensing properties is presented in Table 2. The sensor response (S_R) was calculated as the maximum resistance of thin films after exposure to hydrogen (R_{gas}) to the resistance in pure air (R_{air}), after gas desorption according to the equation:

$$S_R = \frac{R_{gas}}{R_0} \cdot 100\% \tag{6}$$

The response time is the time necessary to reach 90% of the resistance change from resistance in the air to maximum resistance after exposure to gas. In turn, the recovery time is defined in the same way but on the desorption curve. The lowest response time was obtained for the thin film prepared with the 8:1 Ar:O_2 gas ratio. An increase in the response time was observed for samples prepared with a higher O_2 content in the chamber during the deposition process, with all values ranging between 406 and 638 s for those examined at a 120 °C operating temperature and 563 to 668 s for samples measured at a temperature of 150 °C. In turn, the samples deposited with an Ar:O_2 gas ratio 7:1 have the lowest recovery time values for both operating temperatures. The sensor response oscillates around 102.0 to 103.8 for all prepared thin films. A higher sensor response was demonstrated for an operating temperature of 150 °C for all the prepared thin films.

Table 2. Summary of the gas sensing properties.

Ar:O_2 Ratio	Working Temperature (°C)	Response Time (s)	Recovery Time (s)	Sensor Response S_R (%)
8:1	150	563	449	102.9–103.0
	120	406	308	102.3–102.6
7:1	150	598	452	102.7–102.8
	120	638	217	102.0–102.4
6:1	150	668	416	103.0–103.8
	120	581	440	102.2–102.4

The largest obstacles in hydrogen sensing investigations are the slow response and recovery times, which require a high operating temperature, while at room temperature

the detection of a low concentration of hydrogen is weak [62]. In our work, a relatively low operating temperature was obtained, which can be considered an achievement.

3.5. Nanoindentation Measurements

The results of the hardness measurements and the dependence of the hardness of vanadium oxide thin films on the Ar:O_2 gas ratio during the sputtering process are shown in Figure 13. The hardness gradually decreased with a decrease in the argon content in the sputtering gas ratio from about 2.1 GPa to 0.3 GPa. In the literature, reports on the mechanical properties of vanadium oxides are scarce and determined hardness values vary greatly depending on the method of deposition and microstructure [63,64]. Porwal et al. [63] reported that the hardness of vanadium oxide thin films was equal to 0.2 GPa, which is similar to the values obtained in this work for films deposited with an Ar:O_2 ratio of 2:1. In turn, Fateh et al. [64] reported that additional annealing at 300 °C caused the transition from the amorphous to polycrystalline phase of V_2O_5 films and a simultaneous increase in hardness from 3.2 GPa to even 6.4 GPa. In the case of this work, the SEM cross-sections, shown as insets in Figure 13b, revealed that the thin films deposited with low oxygen content in the sputtering atmosphere were densely packed and were very smooth. In turn, in the case of the films deposited with high oxygen content, the cross-sections appear more porous and are, therefore, softer.

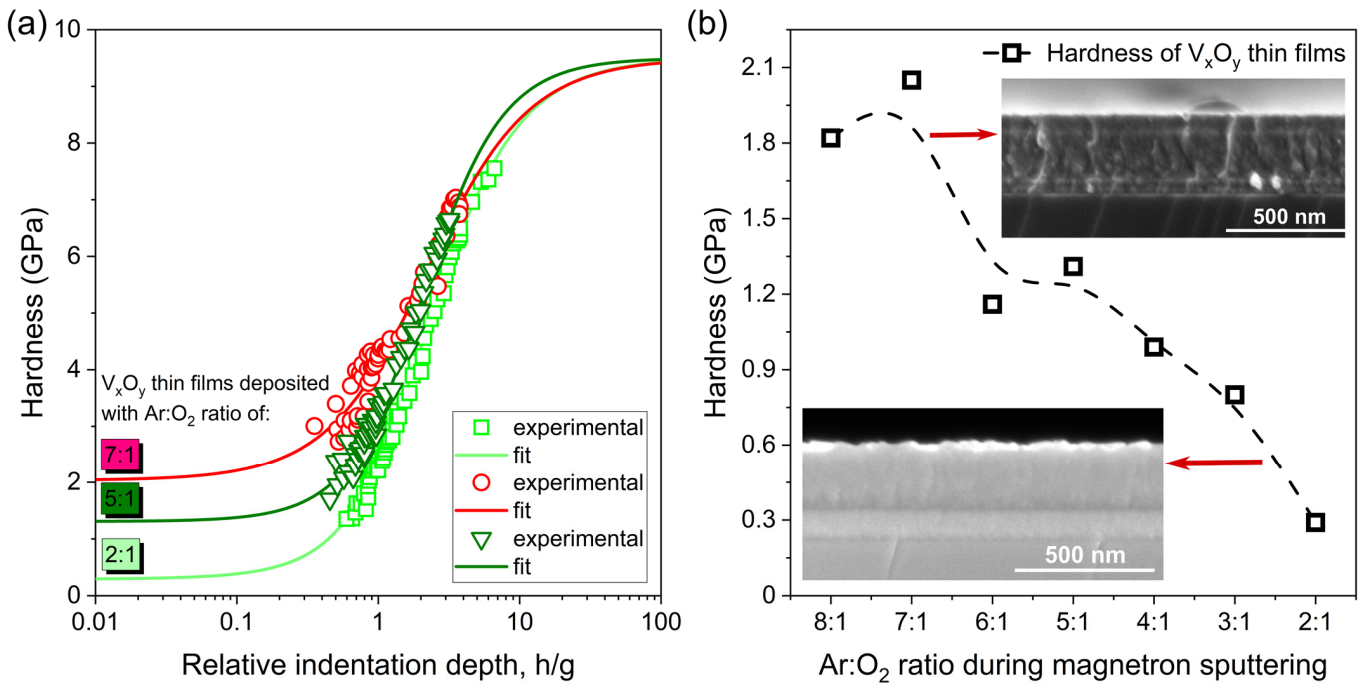

Figure 13. Results of (**a**) the hardness measurement for selected thin films and (**b**) the dependence of hardness of vanadium oxide thin films on the Ar:O_2 gas ratio during the sputtering process.

4. Conclusions

In this work, vanadium oxide thin films were deposited by gas impulse magnetron sputtering with the same conditions, except for varying ratios of the working gas (Ar) and reactive gas (O_2) that were in the range of 8:1 to 2:1. Because of the low temperature of the substrates during the sputtering process, the deposited coatings were amorphous, which was favorable in the case of analysis of other properties; i.e., there was no influence of the structure on the optical, electrical, gas sensing, and nanomechanical properties. It was shown that changing the gas ratio during the deposition process leads to a change in the transparency of the thin films from ca. 51% to 22% with an increase in argon in the gas composition. However, such large changes in the gas ratio, i.e., from 2:1 to 8:1,

did not strongly influence the optical energy band gap. In turn, in the case of electrical properties, all the thin films had semiconducting characteristics and could be categorized as transparent oxide semiconducting (TOS) materials. Taking into consideration their average transparency in the visible wavelength range and resistivity, it was found that thin films with the best merit of figure were deposited with a rather low Ar:O_2 ratio of 3:1. It is also interesting that samples deposited with a high Ar:O_2 ratio were *p*-type semiconductors, while decreasing the gas ratio during sputtering resulted in a change to the electron conduction type. Moreover, gas-sensing measurements in the diluted hydrogen showed that the *p*-type thin films had a better response than the *n*-type samples. Hardness was also shown to gradually decrease with a decrease in the Ar:O_2 gas ratio during the sputtering process. In summary, it is worth highlighting that, with careful control of the sputtering atmosphere, it is possible to obtain amorphous vanadium oxides with specified optical and electrical properties. Increasing the argon content in the gas ratio leads to the deposition of p-type thin films with visible gas sensing properties towards diluted hydrogen and high hardness, while increasing the oxygen content produces thin films with high transparency, good resistivity and a high figure of merit. Further studies will focus on the determination of the oxidation state of each thin film and investigating the influence of post-process annealing on their properties.

Author Contributions: Conceptualization, M.M.; methodology, M.M. and A.L.; formal analysis, M.M., A.L. and J.D.; investigation, M.M., A.L. and D.W.; resources, M.M.; data curation, M.M. and A.L.; writing—original draft preparation, M.M., A.L., J.D. and D.W.; writing—review and editing, M.M. and A.L.; visualization, M.M.; supervision, M.M.; project administration, M.M.; funding acquisition, M.M. All authors have read and agreed to the published version of the manuscript.

Funding: This work was co-financed from the sources given by the Polish National Science Centre (NCN) as a research project number UMO-2020/39/D/ST5/00424 in the years 2021–2024.

Institutional Review Board Statement: Not applicable.

Informed Consent Statement: Not applicable.

Data Availability Statement: The data presented in this study are available on request from the corresponding author.

Acknowledgments: The authors would like to thank Małgorzata Kalisz for the hardness measurements of deposited thin films.

Conflicts of Interest: The authors declare no conflict of interest.

References

1. Hamrit, S.; Djessas, K.; Medjnoun, K.; Bouchama, I.; Saeed, M.A. Realization of High Transparent Conductive Vanadium-Doped Zinc Oxide Thin Films onto Flexible PEN Substrates by RF-Magnetron Sputtering Using Nanopowders Targets. *Ceram. Int.* **2021**, *47*, 22881–22888. [CrossRef]
2. Mehmood, A.; Haidry, A.A.; Long, X.; Zhang, X. Influence of Applied Voltage on Optimal Performance and Durability of Tungsten and Vanadium Oxide Co-Sputtered Thin Films for Electrochromic Applications. *Appl. Surf. Sci.* **2021**, *536*, 147873. [CrossRef]
3. Mallick, A.; Ghosh, S.; Basak, D. Highly Conducting and Transparent Low-E Window Films with High Figure of Merit Values Based on RF Sputtered Al and In Co-Doped ZnO. *Mater. Sci. Semicond. Process.* **2020**, *119*, 105240. [CrossRef]
4. Krishna, M.G.; Debauge, Y.; Bhattacharya, A.K. X-ray Photoelectron Spectroscopy and Spectral Transmittance Study of Stoichiometry in Sputtered Vanadium Oxide Films. *Thin Solid Films* **1998**, *312*, 116–122. [CrossRef]
5. Lee, S.; Ivanov, I.N.; Keum, J.K.; Lee, H.N. Epitaxial Stabilization and Phase Instability of VO_2 Polymorphs. *Sci. Rep.* **2016**, *6*, 19621. [CrossRef]
6. Zhu, M.; Zhang, D.; Jiang, S.; Liu, S.; Qi, H.; Yang, Y. Phase Evolution and Thermochromism of Vanadium Oxide Thin Films Grown at Low Substrate Temperatures during Magnetron Sputtering. *Ceram. Int.* **2021**, *47*, 15491–15499. [CrossRef]
7. Vu, T.D.; Liu, S.; Zeng, X.; Li, C.; Long, Y. High-Power Impulse Magnetron Sputtering Deposition of High Crystallinity Vanadium Dioxide for Thermochromic Smart Windows Applications. *Ceram. Int.* **2020**, *46*, 8145–8153. [CrossRef]
8. Nag, J.; Haglund, R.F. Synthesis of Vanadium Dioxide Thin Films and Nanoparticles. *J. Condens. Matter Phys.* **2008**, *20*, 264016. [CrossRef]
9. Wruck, D.; Ramamurthi, S.; Rubin, M. Sputtered Electrochromic V_2O_5 Films. *Thin Solid Films* **1989**, *182*, 79–86. [CrossRef]

10. Schneider, K.; Lubecka, M.; Czapla, A. V_2O_5 Thin Films for Gas Sensor Applications. *Sens. Actuators B* **2016**, *236*, 970–977. [CrossRef]
11. Zhuiykov, S.; Wlodarski, W.; Li, Y. Nanocrystalline V_2O_5–TiO_2 Thin-Films for Oxygen Sensing Prepared by Sol–Gel Process. *Sens. Actuators B* **2001**, *77*, 484–490. [CrossRef]
12. Yan, W.; Hu, M.; Wang, D.; Li, C. Room Temperature Gas Sensing Properties of Porous Silicon/V_2O_5 Nanorods Composite. *Appl. Surf. Sci.* **2015**, *346*, 216–222. [CrossRef]
13. Jin, W.; Yan, S.; An, L.; Chen, W.; Yang, S.; Zhao, C.; Dai, Y. Enhancement of Ethanol Gas Sensing Response Based on Ordered V_2O_5 Nanowire Microyarns. *Sens. Actuators B* **2015**, *206*, 284–290. [CrossRef]
14. Rizzo, G.; Arena, A.; Bonavita, A.; Donato, N.; Neri, G.; Saitta, G. Gasochromic Response of Nanocrystalline Vanadium Pentoxide Films Deposited from Ethanol Dispersions. *Thin Solid Films* **2010**, *518*, 7124–7127. [CrossRef]
15. Dong, X.; Su, Y.; Wu, Z.; Xu, X.; Xiang, Z.; Shi, Y.; Chen, W.; Dai, J.; Huang, Z.; Wang, T.; et al. Reactive Pulsed DC Magnetron Sputtering Deposition of Vanadium Oxide Thin Films: Role of Pulse Frequency on the Film Growth and Properties. *Appl. Surf. Sci.* **2021**, *562*, 150138. [CrossRef]
16. Chen, Z.; Gao, Y.; Kang, L.; Du, J.; Zhang, Z.; Luo, H.; Miao, H.; Tan, G. VO_2-Based Double-Layered Films for Smart Windows: Optical Design, All-Solution Preparation and Improved Properties. *Sol. Energy Mater. Sol. Cells* **2011**, *95*, 2677–2684. [CrossRef]
17. Soltani, M.; Chaker, M.; Haddad, E.; Kruzelesky, R. 1×2 Optical Switch Devices Based on Semiconductor-to-Metallic Phase Transition Characteristics of VO_2 Smart Coatings. *Meas. Sci. Technol.* **2006**, *17*, 1052–1056. [CrossRef]
18. Ishizaki, H.; Nakajima, T.; Shinoda, K.; Tohyama, S.; Kurashina, S.; Miyoshi, M.; Sasaki, T.; Tsuchiya, T. Improvement of Temperature Coefficient of Resistance of a VO_2 Film on an SiN/Polyimide/Si Substrate by Excimer Laser Irradiation for IR Sensors. *Jpn. J. Appl. Phys.* **2014**, *53*, 05FB15. [CrossRef]
19. Ren, W.; Huang, W.; Zhu, H.; Wang, D.; Zhu, L.G.; Shi, Q. Flexible VO_2/Mica Thin Films with Excellent Phase Transition Properties Fabricated by RF Magnetron Sputtering. *Vacuum* **2021**, *192*, 110407. [CrossRef]
20. Qiao, Y.; Chen, J.; Lu, Y.; Yang, X.; Yang, H.; Xu, K. Fabrication of Low Phase Transition Temperature Vanadium Oxide Films by Direct Current Reactive Magnetron Sputtering and Oxidation Post-Anneal Method. *Infrared Phys. Technol.* **2014**, *67*, 126–130. [CrossRef]
21. Juan, P.C.; Lin, K.C.; Lin, C.L.; Tsai, C.A.; Chen, Y.C. Low Thermal Budget Annealing for Thermochromic VO_2 Thin Films Prepared by High Power Impulse Magnetron Sputtering. *Thin Solid Films* **2019**, *687*, 137443. [CrossRef]
22. Bukhari, S.A.; Kumar, S.; Kumar, P.; Gumfekar, S.P.; Chung, H.J.; Thundat, T.; Goswami, A. The Effect of Oxygen Flow Rate on Metal–Insulator Transition (MIT) Characteristics of Vanadium Dioxide (VO_2) Thin Films by Pulsed Laser Deposition (PLD). *Appl. Surf. Sci.* **2020**, *529*, 146995. [CrossRef]
23. Fieldhouse, N.; Pursel, S.M.; Horn, M.W.; Bharadwaja, S.S.N. Electrical Properties of Vanadium Oxide Thin Films for Bolometer Applications: Processed by Pulse Dc Sputtering. *J. Phys. D Appl. Phys.* **2009**, *42*, 055408. [CrossRef]
24. Luo, Z.; Wu, Z.; Xu, X.; Wang, T.; Jiang, Y. Electrical and Optical Properties of Nanostructured VO_X Thin Films Prepared by Direct Current Magnetron Reactive Sputtering and Post-Annealing in Oxygen. *Thin Solid Films* **2011**, *519*, 6203–6207. [CrossRef]
25. Jang, W.L.; Lu, Y.M.; Lu, Y.R.; Chen, C.L.; Dong, C.L.; Chou, W.C.; Chen, J.L.; Chan, T.S.; Lee, J.F.; Pao, C.W.; et al. Effects of Oxygen Partial Pressure on Structural and Gasochromic Properties of Sputtered VO_x Thin Films. *Thin Solid Films* **2013**, *544*, 448–451. [CrossRef]
26. Koussi, E.K.; Bourquard, F.; Tite, T.; Jamon, D.; Garrelie, F.; Jourlin, Y. Synthesis of Vanadium Oxides by Pulsed Laser Deposition and Rapid Thermal Annealing. *Appl. Surf. Sci.* **2020**, *521*, 146267. [CrossRef]
27. Li, J.; An, Z.; Zhang, W.; Hui, L.; Qin, Z.; Feng, H. Thermochromatic Vanadium Dioxide (VO_2) Thin Films Synthesized by Atomic Layer Deposition and Post-Treatments. *Appl. Surf. Sci.* **2020**, *529*, 147108. [CrossRef]
28. Rupp, J.A.J.; Janod, E.; Besland, M.P.; Corraze, B.; Kindsmüller, A.; Querré, M.; Tranchant, J.; Cario, L.; Dittmann, R.; Waser, R.; et al. Competition between V_2O_3 Phases Deposited by One-Step Reactive Sputtering Process on Polycrystalline Conducting Electrode. *Thin Solid Films* **2020**, *705*, 138063. [CrossRef]
29. Thornton, J.A. The Microstructure of Sputter-Deposited Coatings. *J. Vac. Sci. Technol. A* **1986**, *4*, 3059–3065. [CrossRef]
30. Mazur, M.; Wojcieszak, D.; Wiatrowski, A.; Kaczmarek, D.; Lubańska, A.; Domaradzki, J.; Mazur, P.; Kalisz, M. Analysis of Amorphous Tungsten Oxide Thin Films Deposited by Magnetron Sputtering for Application in Transparent Electronics. *Appl. Surf. Sci.* **2021**, *570*, 151151. [CrossRef]
31. De Castro, M.S.B.; Ferreira, C.L.; de Avillez, R.R. Vanadium Oxide Thin Films Produced by Magnetron Sputtering from a V_2O_5 Target at Room Temperature. *Infrared Phys. Technol.* **2013**, *60*, 103–107. [CrossRef]
32. Tashtoush, N.; Tashtoush, N.M.; Kasasbeh, O. Optical Properties of Vanadium Pentoxide Thin Films Prepared by Thermal Evaporation Method Optical Properties of Vanadium Pentoxide. *Jordan J. Pharm. Sci.* **2013**, *6*, 7–15.
33. Ghanashyam Krishna, M.; Bhattacharya, A. *B* Effect of Thickness on the Optical Absorption Edge of Sputtered Vanadium Oxide Films. *Mater. Sci. Eng. B* **1997**, *49*, 166–171. [CrossRef]
34. Ramana, C.V.; Smith, R.J.; Hussain, O.M. Grain Size Effects on the Optical Characteristics of Pulsed-Laser Deposited Vanadium Oxide Thin Films. *Phys. Status Solidi A* **2003**, *199*, R4–R6. [CrossRef]
35. Benmoussa, M.; Ibnouelghazi, E.; Bennouna, A.; Ameziane, E.L. Structural, Electrical and Optical Properties of Sputtered Vanadium Pentoxide Thin Films. *Thin Solid Films* **1995**, *265*, 22–28. [CrossRef]

36. Kenny, N.; Kannewurf, C.R.; Whitmore, D.H. Optical Absorption Coefficients of Vanadium Pentoxide Single Crystals. *J. Phys. Chem. Solids* **1966**, *27*, 1237–1246. [CrossRef]
37. Cogan, S.F.; Nguyen, N.M.; Perrotti, S.J.; Rauh, R.D. Optical Properties of Electrochromic Vanadium Pentoxide. *J. Appl. Phys.* **1989**, *66*, 1333–1337. [CrossRef]
38. Clauws, P.; Vennik, J. Optical Absorption of Defects in V_2O_5 Single Crystals: As-Grown and Reduced V_2O_5. *Phys. Status Solidi B* **1974**, *66*, 553–560. [CrossRef]
39. Tashtoush, N.M.; Sheiab, A.; Jafar, M.; Momani, S. Determining Optical Constants of Sol-Gel Vanadium Pentoxide Thin Films Using Transmittance and Reflectance Spectra. *Int. J. Appl. Sci.* **2019**, *2*, 59–64. [CrossRef]
40. Pooyodying, P.; Son, Y.H.; Sung, Y.M.; Ok, J.W. The Effect of Sputtering Ar Gas Pressure on Optical and Electrical Properties of Flexible ECD Device with WO_3 Electrode Deposited by RF Magnetron Sputtering on ITO/PET Substrate. *Opt. Mater.* **2022**, *123*, 111829. [CrossRef]
41. Schneider, K. Optical Properties and Electronic Structure of V_2O_5, V_2O_3 and VO_2. *J. Mater. Sci.–Mater. Electron.* **2020**, *31*, 10478–10488. [CrossRef]
42. Tolhurst, T.M.; Leedahl, B.; Andrews, J.L.; Banerjee, S.; Moewes, A. The Electronic Structure of $'$-V_2O_5: An Expanded Band Gap in a Double-Layered Polymorph with Increased Interlayer Separation. *J. Mater. Chem.* **2017**, *5*, 23694–23703. [CrossRef]
43. Beke, S. A Review of the Growth of V_2O_5 Films from 1885 to 2010. *Thin Solid Films* **2011**, *519*, 1761–1771. [CrossRef]
44. Ramana, C.V.; Hussain, O.M.; Naidu, B.S.; Reddy, P.J. Spectroscopic Characterization of Electron-Beam Evaporated V205 Thin Films. *Thin Solid Films* **1997**, *305*, 219–226. [CrossRef]
45. Chain, E.E. Optical Properties of Vanadium Dioxide and Vanadium Pentoxide Thin Films. *Appl. Opt.* **1991**, *30*, 2782–2787. [CrossRef] [PubMed]
46. Dong, X.; Wu, Z.; Xu, X.; Wang, T.; Jiang, Y. Effects of Duty Cycle and Oxygen Flow Rate on the Formation and Properties of Vanadium Oxide Films Deposited by Pulsed Reactive Sputtering. *Vacuum* **2014**, *104*, 97–104. [CrossRef]
47. Lourenco, A.; Gorenstein, A.; Passerini, S.; Smyrl, W.H.; Fantini, M.C.A.; Tabacniks, M.H. Radio-Frequency Reactively Sputtered VO_x Thin Films Deposited at Different Oxygen Flows. *J. Electrochem. Soc.* **1998**, *145*, 706. [CrossRef]
48. Mohite, S.V.; Rajpure, K.Y. Synthesis and Characterization of Sb Doped ZnO Thin Films for Photodetector Application. *Opt. Mater.* **2014**, *36*, 833–838. [CrossRef]
49. Mustafa Öksüzoğlu, R.; Bilgiç, P.; Yildirim, M.; Deniz, O. Influence of Post-Annealing on Electrical, Structural and Optical Properties of Vanadium Oxide Thin Films. *Opt. Laser Technol.* **2013**, *48*, 102–109. [CrossRef]
50. Choi, S.G.; Seok, H.J.; Rhee, S.; Hahm, D.; Bae, W.K.; Kim, H.K. Magnetron-Sputtered Amorphous V_2O_5 Hole Injection Layer for High Performance Quantum Dot Light-Emitting Diode. *J. Alloys Compd.* **2021**, *878*, 160303. [CrossRef]
51. Zhou, X.; Wu, Y.; Yan, F.; Zhang, T.; Ke, X.; Meng, K.; Xu, X.; Li, Z.; Miao, J.; Chen, J.; et al. Revealing the High Sensitivity in the Metal Toinsulator Transition Properties of the Pulsed Laser Deposited VO_2 Thin Films. *Ceram. Int.* **2021**, *47*, 25574–25579. [CrossRef]
52. Gu, H.; Wang, Z.; Hu, Y. Hydrogen Gas Sensors Based on Semiconductor Oxide Nanostructures. *Sensors* **2012**, *12*, 5517–5550. [CrossRef] [PubMed]
53. Mounasamy, V.; Mani, G.K.; Madanagurusamy, S. Vanadium Oxide Nanostructures for Chemiresistive Gas and Vapour Sensing: A Review on State of the Art. *Microchim. Acta* **2020**, *187*, 253. [CrossRef] [PubMed]
54. Zhao, M.; Ong, C.W. Improved H_2-Sensing Performance of Nanocluster-Based Highly Porous Tungsten Oxide Films Operating at Moderate Temperature. *Sens. Actuators B* **2012**, *174*, 65–73. [CrossRef]
55. Hübner, M.; Simion, C.E.; Tomescu-Stănoiu, A.; Pokhrel, S.; Bârsan, N.; Weimar, U. Influence of Humidity on CO Sensing with P-Type CuO Thick Film Gas Sensors. *Sens. Actuators B* **2011**, *153*, 347–353. [CrossRef]
56. Staerz, A.; Weimar, U.; Barsan, N. Current State of Knowledge on the Metal Oxide Based Gas Sensing Mechanism. *Sens. Actuators B* **2022**, *358*, 131531. [CrossRef]
57. Babar, B.M.; Pisal, K.B.; Mujawar, S.H.; Patil, V.L.; Kadam, L.D.; Pawar, U.T.; Kadam, P.M.; Patil, P.S. Concentration Modulated Vanadium Oxide Nanostructures for NO_2 Gas Sensing. *Sens. Actuators B* **2022**, *351*, 130947. [CrossRef]
58. Shankar, P.; Rayappan, J.B.B. Gas Sensing Mechanism of Metal Oxides: The Role of Ambient Atmosphere, Type of Semiconductor and Gases-A Review. *Sci. Lett. J.* **2015**, *4*, 126.
59. Duc Hoa, N.; An, S.; Dung, N.; Quy, N.; Kim, D. Synthesis of P-Type Semiconducting Cupric Oxide Thin Films and Their Application to Hydrogen Detection. *Sens. Actuators B* **2010**, *146*, 239–244.
60. Wang, G.; Yang, S.; Cao, L.; Jin, P.; Zeng, X.; Zhang, X.; Wei, J. Engineering Mesoporous Semiconducting Metal Oxides from Metal-Organic Frameworks for Gas Sensing. *Coord. Chem. Rev.* **2021**, *445*, 214086. [CrossRef]
61. Duc Hoa, N.; van Quy, N.; Anh Tuan, M.; van Hieu, N. Facile Synthesis of P-Type Semiconducting Cupric Oxide Nanowires and Their Gas-Sensing Properties. *Phys. E Low Dimens. Syst. Nanostruc.* **2009**, *42*, 146–149. [CrossRef]
62. Luo, Y.; Zhang, C.; Zheng, B.; Geng, X.; Debliquy, M. Hydrogen Sensors Based on Noble Metal Doped Metal-Oxide Semiconductor: A Review. *Int. J. Hydrogen Energy* **2017**, *42*, 20386–20397. [CrossRef]

63. Porwal, D.; Esther, C.M.E.; Reddy, I.N.; Sridhara, N.; Yadav, N.P.; Rangappa, D.; Bera, P.; Anandan, C.; Sharma, A.K.; Dey, A. Study of the structural, thermal, optical, electrical and nanomechanical properties of sputtered oxide smart thin films. *RSC Adv.* **2015**, *5*, 35737–35745. [CrossRef]
64. Fateh, N.; Fontalvo, G.A.; Mitterer, C. Structural and mechanical properties of dc and pulsed dc reactive magnetron sputtered V_2O_5 films. *J. Phys. D Appl. Phys.* **2007**, *40*, 7716–7719. [CrossRef]